Cell Metabolism
Article

α/β-Hydrolase Domain-6-Accessible Monoacylglycerol Controls Glucose-Stimulated Insulin Secretion

Shangang Zhao,[1,8] Yves Mugabo,[1,8] Jose Iglesias,[1,8] Li Xie,[2] Viviane Delghingaro-Augusto,[1,6] Roxane Lussier,[1] Marie-Line Peyot,[1] Erik Joly,[1] Bouchra Taïb,[3] Matthew A. Davis,[4] J. Mark Brown,[4,7] Abdelkarim Abousalham,[5] Herbert Gaisano,[2] S.R. Murthy Madiraju,[1,*] and Marc Prentki[1,*]

[1]Molecular Nutrition Unit and Montreal Diabetes Research Center, CRCHUM, and Departments of Nutrition, Biochemistry and Molecular Medicine, Université de Montréal, Montréal H2X 0A9, Canada
[2]Department of Medicine, University of Toronto, Toronto, Ontario M5S 1A8, Canada
[3]Department of Pathology and Cell Biology, Université de Montréal, Montréal H2X 0A9, Canada
[4]Section on Lipid Sciences, Department of Pathology, Wake Forest University School of Medicine, Medical Center Boulevard, Winston-Salem, NC 27157, USA
[5]Organization and Dynamics of Biological Membranes, UMR 5246 ICBMS, CNRS-Université Claude Bernard Lyon 1, Bâtiment Raulin, 43, boulevard du 11 novembre 1918, 69622 Villeurbanne, Cedex, France
[6]Present address: Diabetes and Endocrinology Research Unit, Australian National University Medical School, Garran, ACT, Australia
[7]Present address: Cleveland Clinic Lerner Research Institute, Department of Cellular and Molecular Medicine, 9500 Euclid Avenue, Cleveland, Ohio 44195, USA
[8]Co-first authors
*Correspondence: murthy.madiraju@crchum.qc.ca (S.R.M.M.), marc.prentki@umontreal.ca (M.P.)
http://dx.doi.org/10.1016/j.cmet.2014.04.003

SUMMARY

Glucose metabolism in pancreatic β cells stimulates insulin granule exocytosis, and this process requires generation of a lipid signal. However, the signals involved in lipid amplification of glucose-stimulated insulin secretion (GSIS) are unknown. Here we show that in β cells, glucose stimulates production of lipolysis-derived long-chain saturated monoacylglycerols, which further increase upon inhibition of the membrane-bound monoacylglycerol lipase α/β-Hydrolase Domain-6 (ABHD6). ABHD6 expression in β cells is inversely proportional to GSIS. Exogenous monoacylglycerols stimulate β cell insulin secretion and restore GSIS suppressed by the pan-lipase inhibitor orlistat. Whole-body and β-cell-specific ABHD6-KO mice exhibit enhanced GSIS, and their islets show elevated monoacylglycerol production and insulin secretion in response to glucose. Inhibition of ABHD6 in diabetic mice restores GSIS and improves glucose tolerance. Monoacylglycerol binds and activates the vesicle priming protein Munc13-1, thereby inducing insulin exocytosis. We propose saturated monoacylglycerol as a signal for GSIS and ABHD6 as a negative modulator of insulin secretion.

INTRODUCTION

Insulin is secreted from the pancreatic β cell upon fusion of insulin granules with the plasma membrane (Ashcroft and Rorsman, 2012; Kwan and Gaisano, 2009; MacDonald, 2011), and glucose-stimulated insulin secretion (GSIS) occurs via glucose metabolism in the β cell (MacDonald, 2011; Maechler and Wollheim, 1998; Prentki et al., 2013). Insulin secretion is altered in diabetes, and despite decades of research, the signaling pathways involved in GSIS remain to be defined (Nolan and Prentki, 2008). Glucose metabolism in the β cell elevates ATP, which, by closing potassium channels, triggers an increase in cytosolic Ca^{2+} necessary for insulin granule exocytosis (Prentki and Matschinsky, 1987). However, glucose signaling for insulin exocytosis also occurs via other metabolic coupling factors besides ATP (Henquin, 2011; Jitrapakdee et al., 2010; Maechler and Wollheim, 1998; Prentki and Madiraju, 2012).

The glycerolipid/free fatty acid (GL/FFA) cycle (Nolan et al., 2006a; Nolan and Prentki, 2008) conducts synthesis of glycerolipids, including mono-acylglycerols (MAGs), di-acylglycerols (DAGs), and tri-acylglycerols (TGs) and phospholipids followed by their lipolysis to FFA and glycerol. Lipolysis plays a key role in GSIS (Nolan and Prentki, 2008; Prentki and Madiraju, 2012) by producing a signaling molecule(s) that remains to be defined (Prentki et al., 2013). GSIS is reduced in isolated islets obtained from mice deficient in either adipose triglyceride lipase (Peyot et al., 2009), which hydrolyzes TG to DAG (Nolan and Prentki, 2008), hormone-sensitive lipase (Fex et al., 2009; Peyot et al., 2004), which forms MAG from DAG (Haemmerle et al., 2002), or when DAG lipase (which also forms MAG) is inhibited by RHC80267 (Guenifi et al., 2001). On the basis of these observations, we hypothesized that MAG is a key signal mediating the link between glucose and intracellular fatty acid (FA) signaling and insulin secretion.

If DAG were a signal for GSIS (Eliasson et al., 2008; Green et al., 2009; Kwan et al., 2006), suppression or inhibition of HSL or DAG lipase, which elevates DAG levels, should enhance GSIS instead of reducing it. MAG can be hydrolyzed not only by MAG lipase (MAGL) but also by the recently discovered plasma-membrane-bound enzymes α/β-hydrolase domain-containing 6 (ABHD6), with its catalytic site facing the cytosol and ABHD12 with exterior-facing catalytic site (Blankman et al., 2007). Recent studies suggested a potential role for ABHD6 in the control of

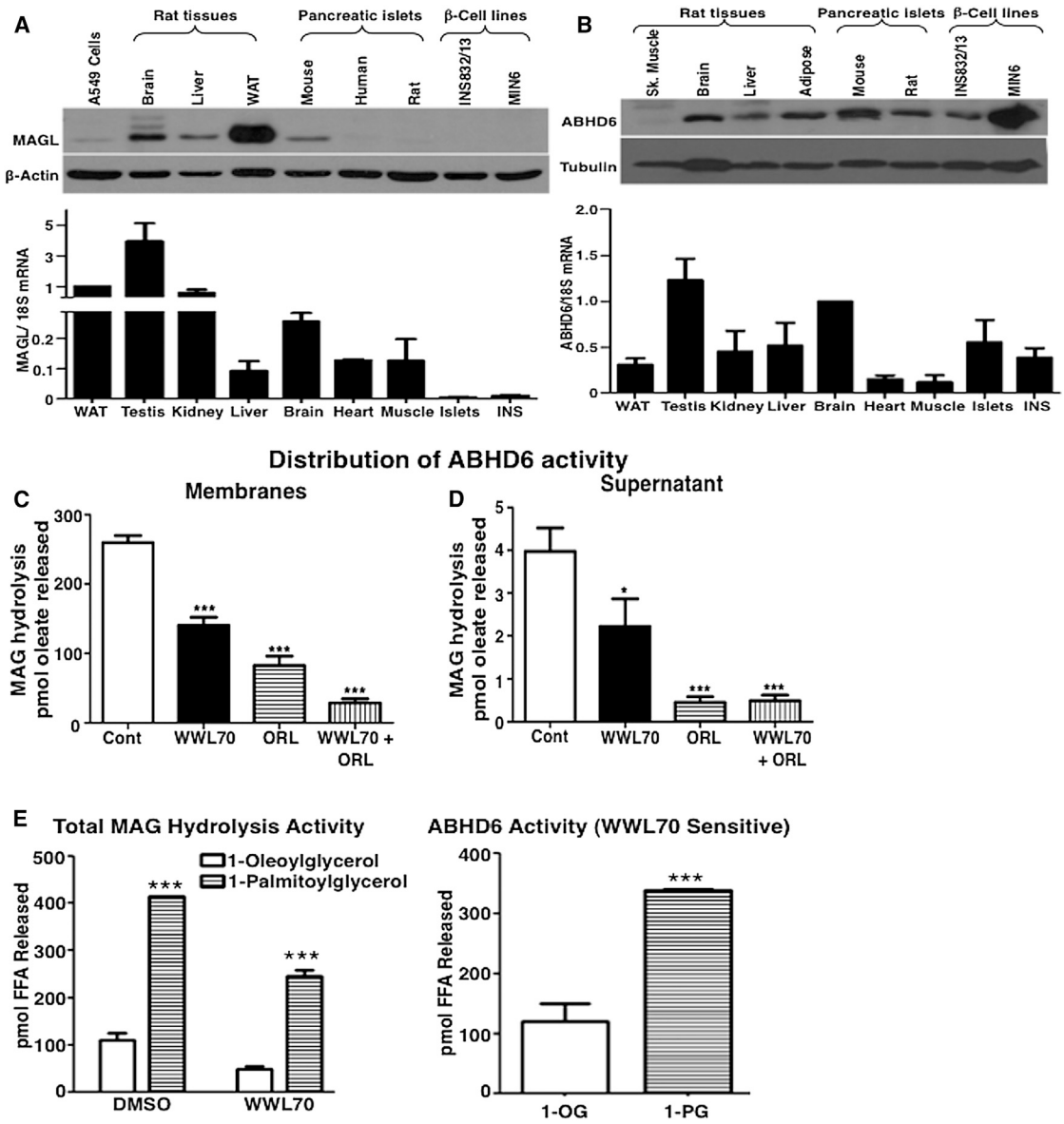

Figure 1. Expression and Distribution of Monoacylglycerol Lipase and ABHD6 in Rat Tissues, Pancreatic Islets, and β Cell Lines

(A) Upper panel: MAGL protein level. Lower panel: MAGL mRNA expression.

(B) Upper panel: ABHD6 protein level. Lower panel: ABHD6 mRNA level.

(C and D) Assessment of MAG hydrolysis using 1-OG (50 μM) as substrate in INS832/13 cells without and with ABHD6 inhibitor WWL70 (10 μM) and panlipase inhibitor orlistat (25 μM) in (C) membranes and (D) cytosol. n = 6. *p < 0.05; ***p < 0.001 versus control (Cont).

(E) WWL70-sensitive MAG hydrolysis activity in INS832/13 cell extracts is higher with 1-PG (50 μM) than with 1-OG (50 μM). ***p < 0.001 versus 1-OG (n = 3). All the values shown are mean ±SEM.

metabolic syndrome (Thomas et al., 2013) and inflammation (Alhouayek et al., 2013).

Here we show that glucose stimulation elevates various MAG species in the β cells, particularly saturated 1-MAG species, and that MAG accessible to ABHD6 but not to MAGL acts as a signal for promoting insulin granule exocytosis by binding to the vesicle priming protein Munc13-1. Suppression of ABHD6 either genetically or pharmacologically leads to MAG buildup in β cells with a resultant increase in GSIS in vitro, ex vivo, and in vivo. The data indicate that ABHD6 negatively regulates GSIS and that MAG is a metabolic coupling factor for insulin secretion in response to glucose and FAs.

RESULTS

Membrane-Bound ABHD6 Is the Predominant MAG Lipase in β cells

In β cell lines and islets from rat, mouse, and human, MAGL is expressed at very low levels, unlike other tissues (Figure 1A). However, ABHD6 is well expressed both at mRNA and protein

levels in islets and β cell lines (Figure 1B). Using 1-oleoylglycerol (1-OG), MAG hydrolase activity in INS832/13 β cells was found primarily in the membrane fraction (Figure 1C) and is inhibited by the ABHD6 inhibitor WWL70, which does not affect MAGL, ATGL, or HSL (Bachovchin et al., 2010; Blankman et al., 2007), and by panlipase inhibitor orlistat (Figure 1D). ABHD6 activity in INS832/13 cell extracts with 1-palmitoylglycerol (1-PG) is ~3-fold higher than with 1-OG (Figure 1E). ABHD12 expression is low in β cells and rodent islets as compared to human islets (data not shown).

Elevation of 1-MAG by Glucose and ABHD6 Inhibition in β Cells Correlates with GSIS

If MAG is a mediator of GSIS, its level is expected to respond to an increase in glucose concentration, and agents that either increase or reduce MAG levels should modulate insulin secretion accordingly. Incorporation of [1-^{14}C]-arachidonic acid into 1- and 2-MAG, besides other glycerolipids, increased in INS832/13 cells at high glucose (Figure S1A available online). We also tested the effect of WWL70 and orlistat on [^{14}C]-glucose incorporation into different lipids. Under conditions where the lipid carbons are prelabeled with [^{14}C]-glucose, incubation with 10 mM glucose led to elevated lipolysis, measured as ^{14}C-FFA release (Figure S1B) and a rise in neutral glycerolipids, particularly 1- and 2- MAG (Figure S1C). TG accumulated with orlistat but not with WWL70 (Figure S1D), and these inhibitors had no effect on total DAG levels (Figure S1D). While orlistat had no effect on 2-MAG, it was increased by WWL70 (Figure S1C). Orlistat, which inhibits GSIS (Nolan et al., 2006b), decreased 1-MAG, while WWL70, which enhances GSIS (see below Figure 3), increased 1-MAG (Figure S1C). Thus, elevated glucose promotes lipolysis and FFA release in β cells and causes a rise in 1- and 2-MAG levels that is amplified in the presence of WWL70. In addition, GSIS in the presence of inhibitors of lipolysis (orlistat) or ABHD6 (WWL70) correlates only with 1-MAG and not 2-MAG, DAG, or TG.

Glucose Specifically Increases Saturated Long-Chain FA and MAG Species

As ABHD6 inhibition reduced glucose-induced FFA release from INS cells (Figure S1B), we examined if this is specific for any particular FFA. In rat islets, 16.7 mM glucose specifically increased the release of long-chain saturated FFA (Figure 2A)—e.g., palmitate (C16:0) and stearate (C18:0)—and this was abolished by WWL70 (Figure 2B), but the release of unsaturated FFA or saturated FFA of <C16 chain length was not affected (Figures 2A and 2B). Similar changes were noticed in the total FFA present in the islets (Figure 2C). Thus, WWL70 is a useful tool to study the role of ABHD6 and MAG in glucose signaling as it shows the anticipated effects on lipid metabolism. It reduces MAG hydrolysis in vitro, increases MAG levels, and reduces FFA content and release in intact β cells.

The pattern of lipolysis (FFA release) with glucose and WWL70 was largely related to the MAG species in the cells. As glucose and WWL70 led to MAG accumulation in INS cells incubated with [^{14}C]-glucose, we examined the effect of WWL70 on individual MAG species (Figure 2D). Thus, a 2–10 mM increase in glucose elevated total cellular MAG (both 1- and 2-MAG) >2-fold, and this was further increased by WWL70 (Figure 2E). Glucose primarily increased both 1- and 2-PG (Figure 2F) and SG (Figure 2G), though there was noticeable effect on other MAGs. WWL70 was specific in further elevating the 1-MAG levels, in particular 1-PG and 1-stearoylglycerol (1-SG) (Figures 2F and 2G), and other saturated FA-containing MAGs (Figure 2D). This indicates that ABHD6 has preferential access to 1-MAGs with saturated FA.

MAG Enhances Insulin Release and Restores GSIS Suppressed by Orlistat

Since glucose primarily elevates long-chain saturated MAG, we tested whether these MAGs are efficient secretagogues when added exogenously. 1-PG and 1-SG were most effective in enhancing GSIS in INS832/13 cells (Figure 3A), compared to 1-OG (Figure 3A) and 1-linoleoylglycerol (Figure S2A). The GSIS enhancing effect by 1-PG (Figure 3B) and 1-SG (Figure S2B) was also seen in human and rat islets.

Exogenous MAG (1-PG, Figure 3C; 1-SG, Figure S2C; and 2-arachidonoylglycerol, Figures S2D, S2E, and S2F) was not only effective in enhancing GSIS but also in restoring GSIS suppressed by orlistat in INS832/13 cells. This provides strong pharmacological evidence for the view that lipolysis-derived MAG is a signal for GSIS.

Cannabinoid Receptors Are Not Implicated in Glucose Signaling for Insulin Secretion

A specific antagonist (AM251) of the CB1 receptor (Lan et al., 1999) known to be present in β cell (Matias et al., 2006), and an inverse agonist (AM630) of the CB2 receptor (Ross et al., 1999) whose presence in β cells is controversial (Kim et al., 2011), did not alter GSIS (Figure S2E and S2F). In addition, restoration of orlistat-inhibited GSIS by 2-arachidonoylglycerol (2-AG) was not affected by AM251 (Figure S2F).

ABHD6 Inhibition Amplifies GSIS

Inhibition of ABHD6 by WWL70 in INS832/13 cells, which causes MAG accumulation, almost doubled GSIS both in the presence and absence of palmitate (Figure 3D). In contrast, orlistat, which decreased 1-MAG (Figure S1C), inhibited GSIS (Figure 3D). WWL70 had no effect on insulin secretion at low glucose and amplified only GSIS, with maximal effect at 10 μM (Figure S2G), without affecting the total cellular insulin content (data not shown). WWL70 was also effective in enhancing GSIS in islets from CD1 mice (Figure 3E), C57Bl6 mice, and Wistar rats (data not shown), as well as from nondiabetic human donors (Figure 3E). Insulin secretion induced by membrane depolarization with 10 mM arginine or 35 mM KCl was not affected by WWL70 in INS832/13 cells (data not shown).

Insulin Secretion Is Inversely Proportional to ABHD6 Levels

To further ascertain the role of ABHD6 in GSIS regulation, we modified ABHD6 expression in INS832/13 cells by overexpression or RNAi knockdown. An ~3 fold increase in ABHD6 (Figure 4A) decreased GSIS with or without palmitate (Figure 4B), as compared to GFP-expressing control cells. In contrast, a decrease in ABHD6 content by >80% using two different siRNAs (A1 and A2) led to ~2-fold increase in GSIS, in comparison to control RNAi-transfected cells (Figures 4C, 4D,

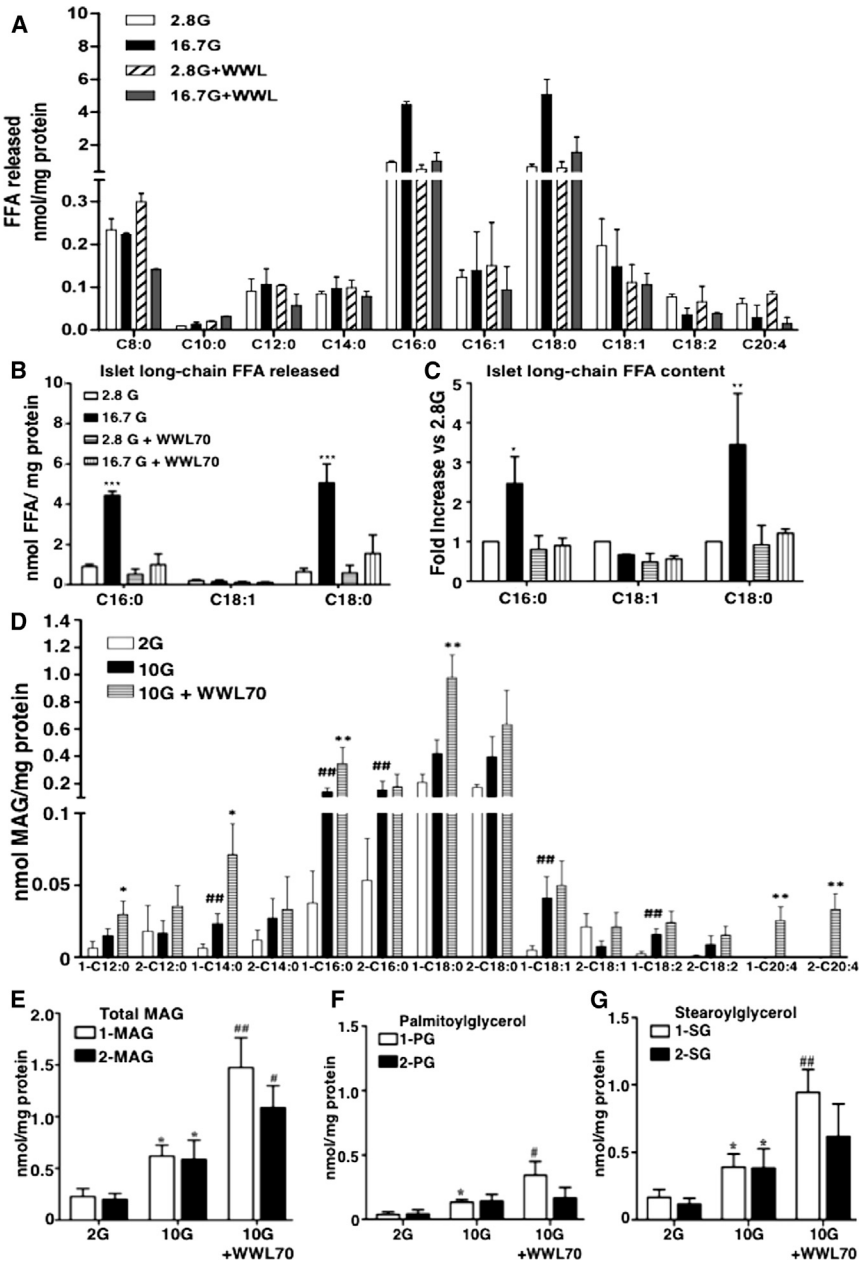

Figure 2. Glucose Specifically Enhances the Production and Release of Saturated FFA from Rat Islets and Increases the Differential Production of Monoacylglycerol Species in β Cells

(A–C) Release and cellular content of different FFA species by isolated rat islets at 2.8 mM glucose (2.8G) and 16.7G with and without 10 μM WWL70 after 2 hr incubation. n = 12. *p < 0.05; **p < 0.01; ***p < 0.001 versus 2.8G.

(B) Release of palmitate (C16:0), stearate (C18:0), and oleate (C18:1) into incubation medium; (C) cellular content of palmitate, oleate, and stearate in rat islets.

(D–G) Effect of glucose and 10 μM WWL70 on the content of MAG species in INS832/13 cells after 2 hr incubation. 2G, 2 mM glucose; 10G, 10 mM glucose.

(D) All measured MAG species; ##p < 0.01 versus 2G; *p < 0.05; **p < 0.01 versus 10G.

(E–G) (E) Total MAG corresponding to the sum of all measured MAG species; (F) 1- and 2- PG (C16:0) and (G) 1- and 2-SG (C18:0). n = 15; *p < 0.05 versus 2G; #p < 0.05; ##p < 0.01 versus 10G. All the values shown are mean ±SEM.

and 4E). An ABHD6 gene expression dosage effect on GSIS with the two siRNAs is apparent.

MAG Hydrolysis by ABHD6 but Not by MAG Lipase Controls Insulin Secretion

We tested whether the signaling competent MAG for insulin secretion is accessible not only to ABHD6 but also to the small amount of MAGL in the β cell. MAGL is distributed between cytosol and membrane fractions (Severson and Hee-Cheong, 1988), unlike ABHD6, which is membrane bound (Blankman et al., 2007) (Figure 1C). Inhibition of MAGL by JZL184 (Long et al., 2009) caused a modest increase in MAG levels in INS832/13 cells but had no effect on GSIS (Figure S3). In addition, RNAi silencing (Figures 4F and 4G) or overexpression of MAGL (Figures 4H and 4I) in INS832/13 cells had no effect on GSIS. Thus, only ABHD6-accessible MAG acts as a signal for GSIS.

Enhanced Insulin Secretion in Whole-Body ABHD6-Deficient Mice

Whole-body ABHD6 deletion in mice was achieved by knockout (KO)-first technique (Figure S4A) (Skarnes et al., 2011). Gene deletion was verified by genotyping. Genomic PCR of *abhd6* locus yielding a single fragment of 517 bp is indicative of gene deletion in the homozygous KO mice, whereas a fragment of 200 bp is indicative of wild-type (WT) (Figure S4B). Both fragments were noticed in heterozygous (HZ) mice. ABHD6 deletion was also confirmed in the western blots showing complete loss of the 37 kDa ABHD6 protein (Figure 5A) in the homozygous KO mice. There was no difference in the growth and food intake of ABHD6-KO and HZ mice in comparison to WT mice up to 25 weeks of age (Figures S4C and S4D).

We examined if the isolated islets from 16-week-old ABHD6-KO mice also exhibit enhanced GSIS and elevated MAG content, similar to the in vitro approaches using WWL70 and RNAi knockdown. These experiments revealed an increase in GSIS in the ABHD6-KO islets at 8.3 and 16.7 mM glucose, while the islets from HZ mice also showed elevated GSIS at 16.7 mM glucose (Figure 5B). Interestingly, KO islets also showed elevated KCl-stimulated insulin secretion (Figure 5B).

We measured MAG content ex vivo, in islets from ABHD6-KO, HZ, and WT mice after incubation at 2.8 and 16.7 mM glucose. Total and 1-MAG (Figures 5C and 5D) were elevated in the islets

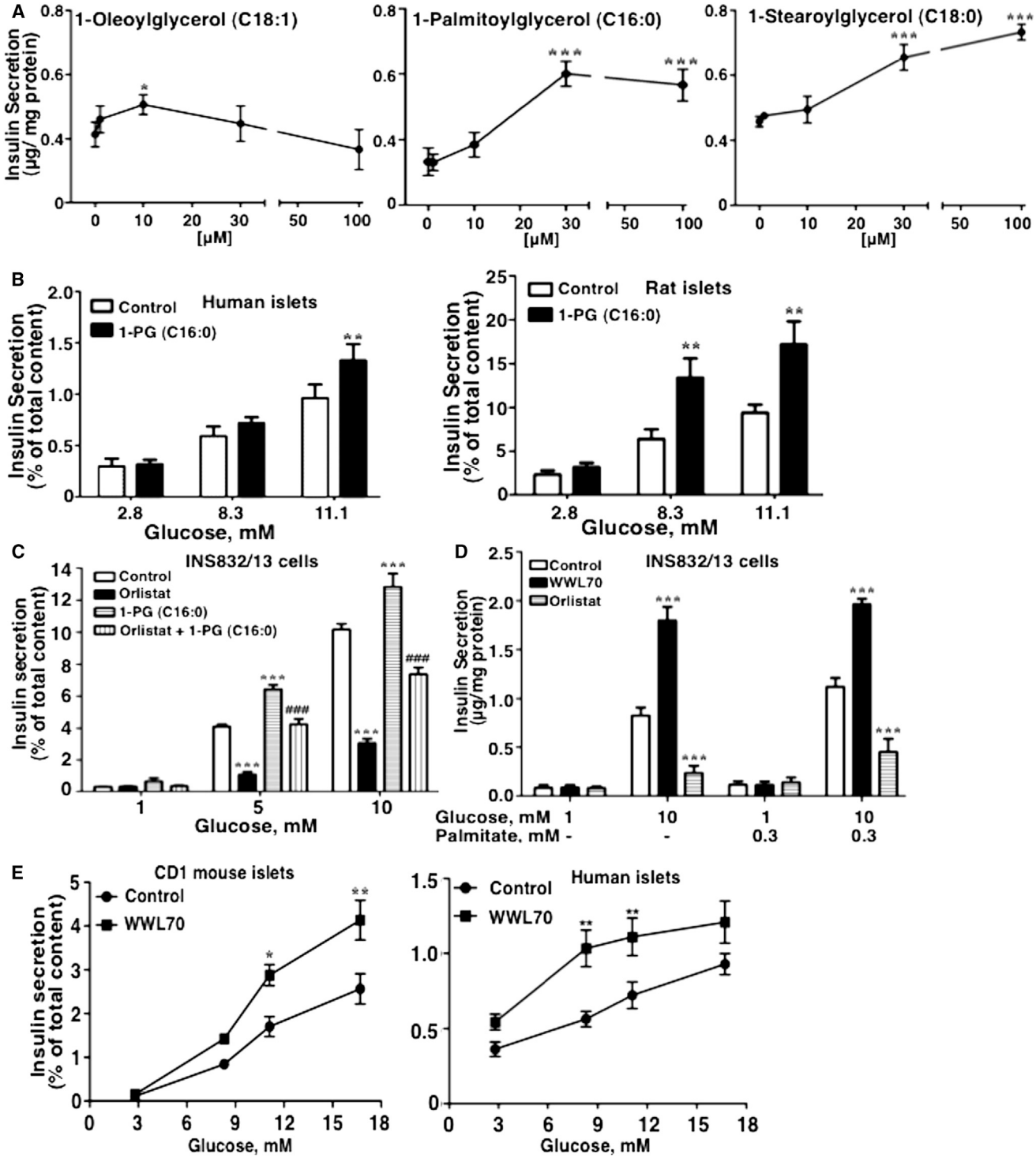

Figure 3. Monoacylglycerol and the ABHD6 Inhibitor WWL70 Enhance Insulin Secretion in β Cells

(A) Dose-dependent effect of different MAGs on GSIS at 5 mM glucose in INS832/13 cells. n = 12. *p < 0.05; ***p < 0.001 versus no MAG addition.

(B) 1-PG (100 μM) enhances GSIS in human islets (n = 4) and rat islets (n = 6). **p < 0.01 versus control.

(C) Exogenous MAG restores GSIS inhibited by orlistat. 1-PG (50 μM) restoration of 25 μM orlistat-inhibited GSIS (at 5 and 10 mM glucose) in INS832/13 cells. n = 12. ***p < 0.001 compared with control; ###p < 0.001 versus the orlistat group.

(D) Effect of WWL70 (10 μM) and orlistat (25 μM) on GSIS in INS832/13 cells. Insulin secretion was measured at 1 and 10 mM glucose without and with 0.3 mM palmitate. n = 12. ***p < 0.001 versus control.

(E) Effect of WWL70 (10 μM) on GSIS in CD1 mouse islets and human islets. n = 12. *p < 0.05; **p < 0.01 versus no WWL70 addition. All the values shown are mean ±SEM.

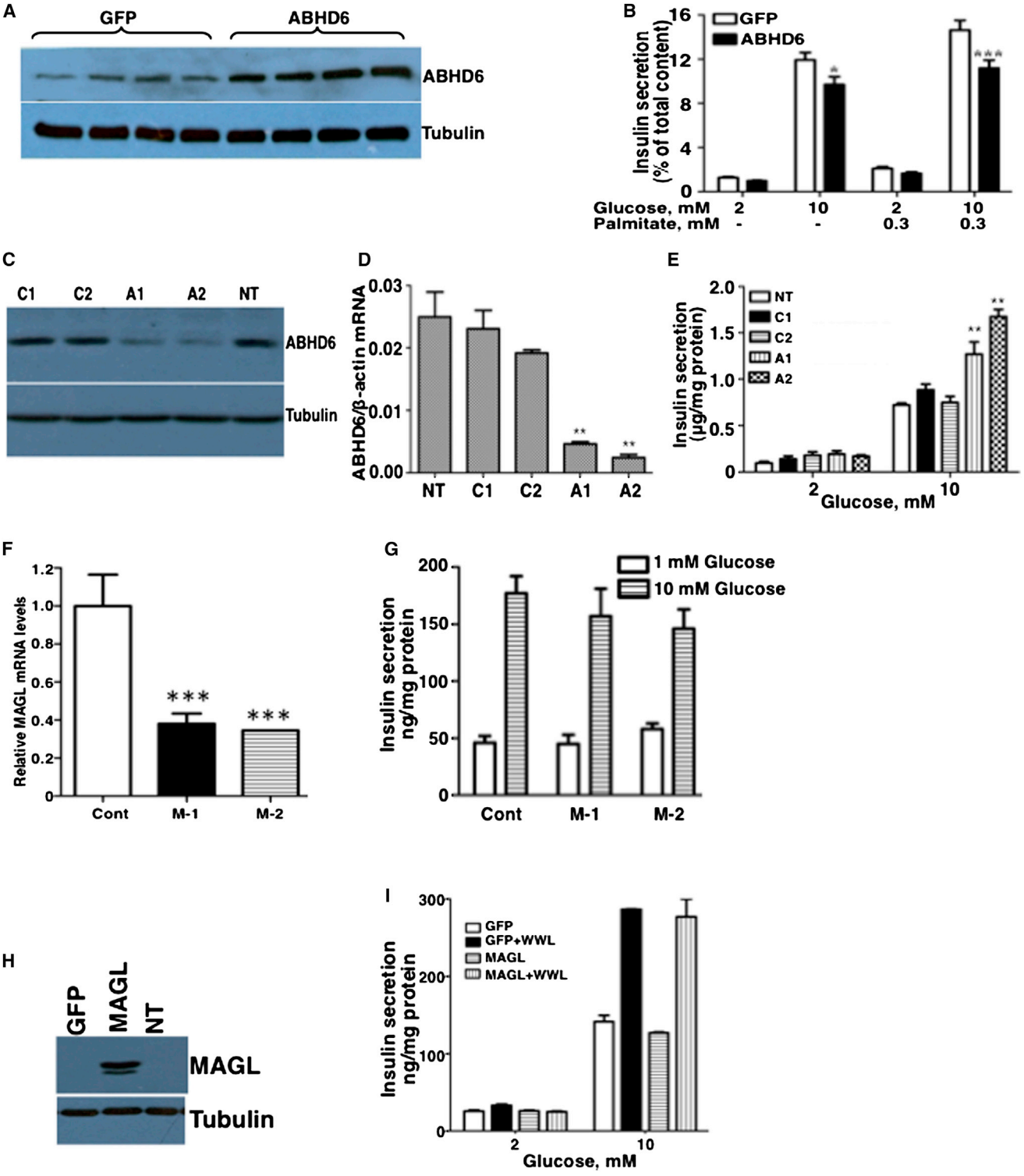

Figure 4. Expression Level of ABHD6 but Not MAGL Affects Glucose-Stimulated Insulin Secretion in β Cells

(A–E) ABHD6 overexpression ([A] and [B]) and RNAi knockdown ([C]–[E]) in INS832/13 cells.

(A) ABHD6 expression in cells transfected with pCMV6-ABHD6 (48 hr posttransfection) as compared to cells expressing GFP.

(B) Insulin secretion in control and ABHD6 overexpressing cells at 2 and 10 mM glucose without and with palmitate. n = 9. *$p < 0.05$; ***$p < 0.001$ versus control cells.

(C) Reduced ABHD6 expression by RNAi knockdown for 24 hr. A1 and A2 siRNAs reduce the protein level as compared to the control siRNAs C1 and C2. NT, not transfected.

(D) Corresponding ABHD6 mRNA levels.

(legend continued on next page)

from all animal types at high glucose. The increase in 2-MAG was moderate and significant only in the KO islets (Figure S4E). Importantly, there was an inverse effect of ABHD6 "gene dosage" on total MAG, 1-MAG, and 2-MAG levels at high glucose (Figures 5C, 5D, and S4E). Thus, genetic deletion of ABHD6 was associated with enhanced ex vivo GSIS and total MAG, as well as 1-MAG and 2-MAG in the islets. Similar to the observations with INS832/13 cells (Figure 2D), maximal changes in the ABHD6-KO islets were seen in saturated-FA-containing MAG species (Figures S4F and S4G). Thus, in ABHD6-KO islets, high glucose induced ~4-fold increase in 1-PG and >2-fold increase in 1-SG and these increases were higher than in WT and HZ islets (Figure S4F). While similar trend was seen in corresponding 2-MAG levels, the total amounts were lower than 1-MAG (Figure S4G). Other 1-and 2-MAGs contributed quantitatively much less to total MAG (data not shown).

We then assessed the impact of ABHD6 deletion on GSIS in vivo by oral glucose tolerance test (OGTT) in 26-week-old male ABDH6-KO and HZ mice and WT littermates. Results indicated unaltered glucose tolerance in both ABHD6-KO and HZ mice, as compared to WT mice (Figure 5E). Plasma insulin during OGTT increased significantly in both the KO and HZ mice (Figure 5F; inset showing area under the curve [AUC]), consistent with the results from the normal mice administered with ABHD6 inhibitor WWL70 (see below). The increase in GSIS appeared to be ABHD6 gene dosage dependent, as evident from AUC calculations (Figure 5F inset). Since there was elevated insulinemia with unchanged glycemia in the KO and HZ mice upon glucose load, we tested if the insulin sensitivity is altered in these mice. Hyperinsulinemic euglycemic clamp revealed unaltered insulin sensitivity in KO and HZ mice fed chow diet for 26 weeks (Figure 5G), confirming the results obtained by insulin tolerance test, (Figure S4H). Basal glycemia and insulinemia were similar in the KO, HZ, and WT mice.

Lack of Effect of WWL70 on GSIS and MAG Hydrolyzing Activity in ABHD6-KO Islets

ABHD6-KO mouse islet extracts showed ~50% reduced MAG hydrolytic activity that was insensitive to inhibition by WWL70, unlike in the WT islets (Figure S4I). The residual MAG hydrolysis activity in the KO-islet extracts could be due to HSL, MAGL, and other nonspecific hydrolases. ABHD6 inhibition by WWL70 enhanced GSIS in WT islets ex vivo but not in whole-body KO mouse islets, which show already enhanced GSIS (Figure S4J). These results reinforce the view that WWL70 is a specific inhibitor of ABHD6 and that its effect on GSIS in β cells is exclusively due to ABHD6 inhibition.

ABHD6 Inhibition Enhances GSIS and Restores Glucose Tolerance in Diabetic Mice

We examined if the GSIS-enhancing effect of ABHD6 inhibition is noticeable in vivo in control CD1 mice and in the low-dose streptozotocin (LD-STZ) diabetes mouse model. We chose to employ the LD-STZ mouse model as this presents with ~50% reduced β cell mass, fed hyperglycemia of approximately 20 mM, slightly elevated fasting glycemia, and significantly lowered fed insulinemia (Hayashi et al., 2006). Thus, in order to study the in vivo effects of ABHD6 inhibition specifically on insulin secretion, we felt it important to choose an animal model that is not insulin resistant and hyperinsulinemic (e.g., db/db, ob/ob, high-fat-fed mice, etc.) and where β cell mass is not drastically decreased. Intraperitoneal (i.p.) administration of WWL70 for 3 days enhanced insulinemia in control mice during OGTT but did not affect glycemia (Figures 5H and 5I). In LD-STZ diabetic mice WWL70 restored glucose-responsive insulin release, normalized basal glycemia, and markedly improved glucose tolerance (Figures 5J and 5K).

Enhanced GSIS In Vivo and Ex Vivo in β-Cell-Specific ABHD6 KO Mice

In order to ascertain whether the insulin secretion effects seen in whole-body ABHD6-KO mice are indeed due to the lack of ABHD6 in pancreatic β cells per se, we generated β-cell-specific ABHD6 KO (BKO) mice. Floxed ABHD6 mice on pure C57Bl6N background were produced from the KO-first mice (whole-body ABHD6-KO) by crossing with Flpo transgenic mice on pure C57Bl6N genetic background. Floxed ABHD6 mice were crossed with tamoxifen-inducible mip-*cre* transgenic mice (Wicksteed et al., 2010) that were backcrossed to C57Bl6N for eight generations to produce mice that carried floxed ABHD6 gene and tamoxifen-inducible mip-*cre* transgene, which were used for generating BKO mice. After 2 weeks following five consecutive tamoxifen injections, ABHD6 expression was abrogated only in pancreatic islets (β cells) (Figure 6A) but not in other tissues (Figures 6B–6D) of the BKO mice. ABHD6 mRNA levels were unchanged in ventromedial hypothalamus (Figure S5A) and arcuate nucleus (Figure S5B) regions of hypothalamus, indicating no leakage of *cre* expression in these regions and thus there is no central nervous system involvement in the altered β cell function of BKO mice. Similar to whole-body KO mice, there were no significant alterations in body weight gain (Figure S5C) or food intake (Figure S5D) up to 5 weeks post-tamoxifen injection. BKO mice did not show any changes in β cell mass compared to floxed and mip-*cre* control mice (Figure S5E). BKO male mice showed slightly improved glucose tolerance (Figure 6E) and elevated insulinemia (Figure 6F) during OGTT. Similar to the whole-body KO mice, BKO mouse islets showed enhanced GSIS ex vivo (Figure 6G).

MAG Binds to the Exocytosis Effector Munc13-1

Among the potential targets for MAG action relevant for insulin secretion, Munc13-1 seemed plausible, as this protein orchestrates membrane fusion events in various cell types (Ma et al.,

(E) Insulin secretion at 2 and 10 mM glucose in control cells and after RNAi knockdown of ABHD6. **$p < 0.01$ versus control (C1 and C2) groups; n = 9.
(F and G) MAGL RNAi knockdown.
(F) MAGL mRNA levels decreased after RNAi knockdown for 48 hr. M-1 and M-2 are the siRNAs; Cont, RNAi control.
(G) Insulin secretion in INS832/13 cells at 1 and 10 mM glucose after MAGL RNAi knockdown.
(H and I) MAGL overexpression.
(H) Elevated expression of MAGL in INS cells transfected with pCMV6-MAGL (48 hr posttransfection) as compared to GFP-expressing and untransfected cells (NT).
(I) Insulin secretion at 2 and 10 mM glucose without and with 10 μM WWL70; n = 9. All the values shown are mean ±SEM.

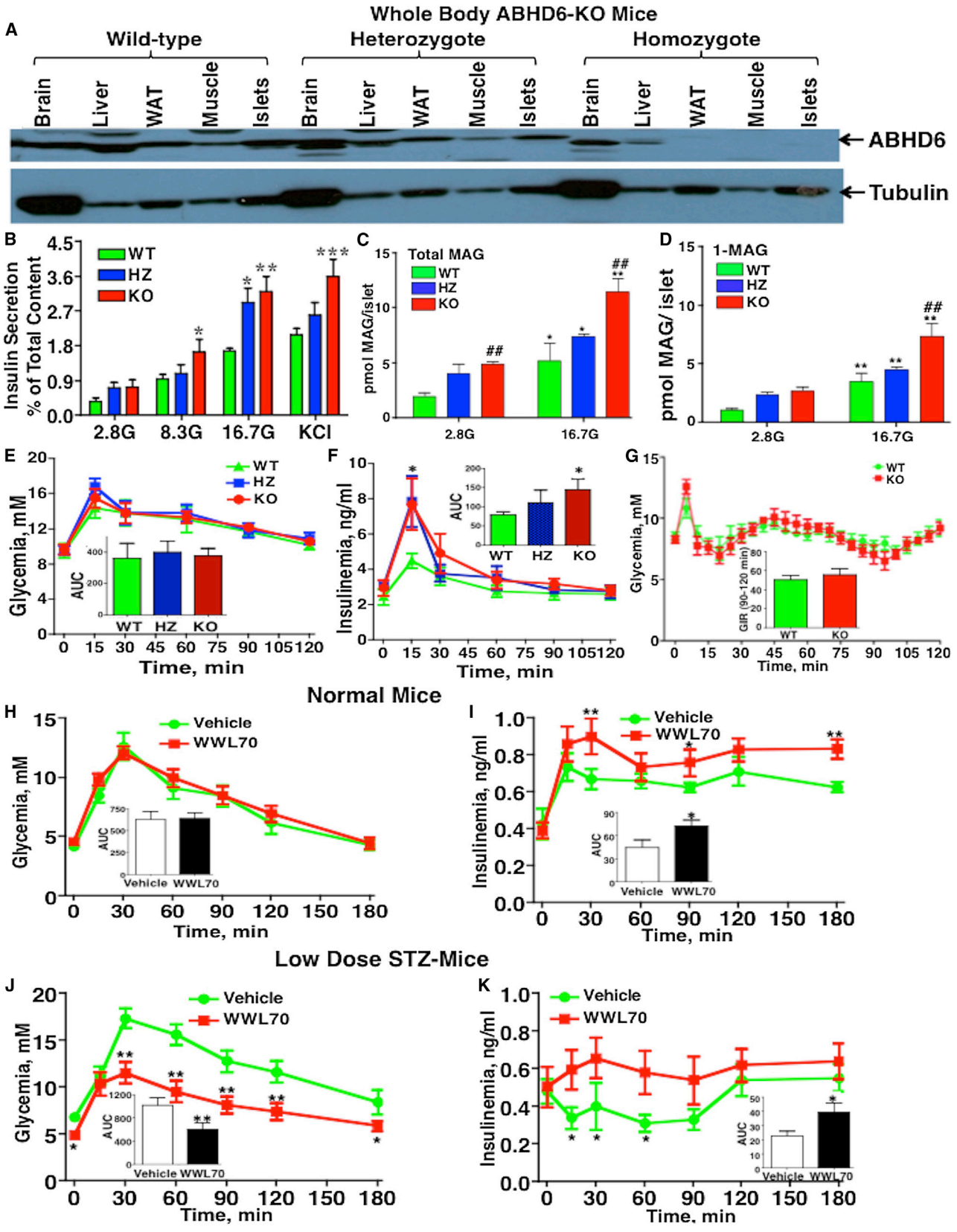

(legend on next page)

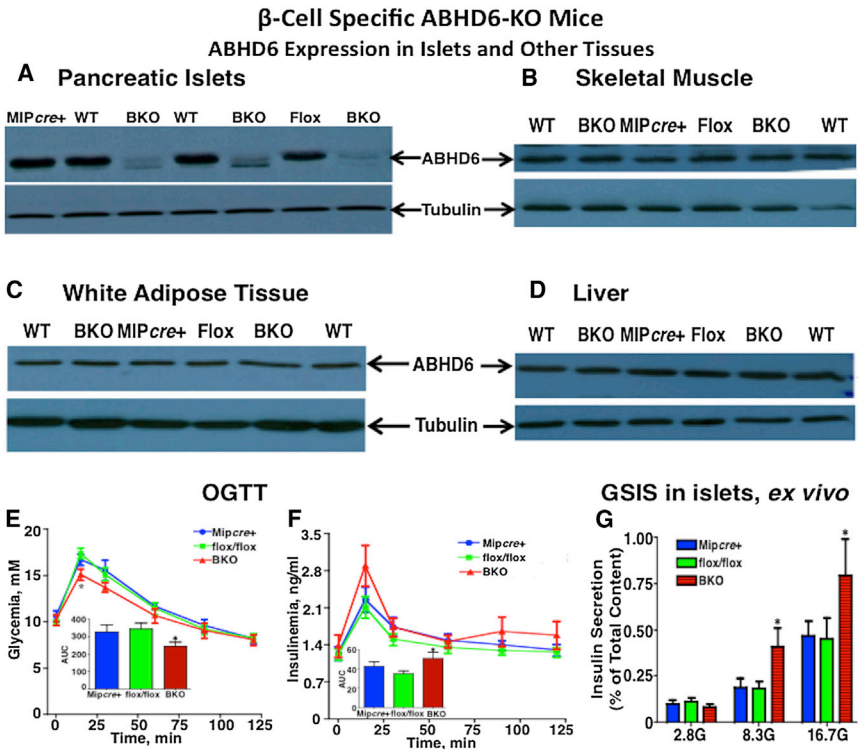

Figure 6. Enhanced Glucose-Induced Insulin Secretion by β-Cell-Specific Deletion of ABHD6 in Mice

(A–D) Expression of ABHD6 protein in different tissues from β-cell-specific ABHD6-KO (BKO) mice. Two weeks post-tamoxifen injection to induce Cre recombinase expression and ABHD6 deletion in β cells, tissues from the mip*cre*+, WT, flox/flox, and BKO mice were analyzed for ABHD6 expression by western blot. (A) Pancreatic islets, (B) skeletal muscle, (C) white adipose (visceral), and (D) liver. Representative blots from two separate experiments.

(E–G) Effect of BKO on glucose tolerance and glucose-induced insulin secretion in vivo and ex vivo in islets.

(E) Glycemia during OGTT in mip*cre*+ (n = 9), flox/flox (n = 12), and BKO (n = 9) mice. OGTT was performed after a 6 hr food withdrawal. Inset depicts AUC. *p < 0.05 versus flox/flox.

(F) Corresponding insulinemia in the OGTT. Inset, AUC for insulinemia. *p < 0.05 versus flox/flox.

(G) Ex vivo GSIS at 2.8, 8.3, and 16.7 mM glucose in islets from mip*cre*+ (n = 7), flox/flox (n = 8), and BKO mice (n = 8). Insulin secretion is shown as percentage of total insulin content. *p < 0.05 versus flox/flox or mip*cre*+. All the values shown are mean ±SEM.

2013), binds DAG, and participates in the exocytotic process in β cells (Kwan and Gaisano, 2009). However, the C1 domain of Munc13-1 shows lower affinity for DAG, the proposed physiological ligand (Rhee et al., 2002), than for phorbol myristate acetate (PMA) (Shen et al., 2005). We assessed if MAG is a better ligand than DAG for Munc13-1 C1 domain. Using three independent approaches, we proved it to be the case. (1) Tryptophan fluorescence quenching of the Munc13-1 C1 domain showed that 1-PG binds as effectively as PMA, a well-known C1 domain ligand, and better than dioctanoylglycerol (Figure 7A). Palmitate did not show any binding. Similar highly efficient binding was also observed with 1-SG (data not shown). (2) Protein-lipid overlay showed that GST-Munc13-C1 fusion protein (but not GST alone) binds to 1-PG and 1-SG, similar to or better than dioctanoylglycerol, whereas binding with palmitate, stearate, and TG was insignificant (Figure 7B). (3) Munc13-1 C1 domain peptide could bind to the NBD-MAG and quench its fluorescence (emission λ = 540 nm), whereas a similar-sized control peptide (glucagon-like peptide 1) could not bind NBD-MAG (Figure S6A).

Glucose and MAG Cause Munc13-1 Translocation to Plasma Membrane

Confocal microscopy (Figure 7C) revealed that in INS832/13 cells expressing Munc13-1-EGFP, high glucose concentration

Figure 5. Enhanced Glucose-Induced Insulin Secretion by Genetic Deletion or Pharmacological Suppression of ABHD6 in Mice

(A) Western blot analysis of different tissues reveals complete loss of ABHD6 protein in homozygous ABHD6-KO mice, a partial loss in heterozygote ABHD6-KO mice as compared to the WT mice.

(B–D) Elevated GSIS in ABHD6-KO mouse islets is associated with glucose-dependent increase in the islet MAG content.

(B) Ex vivo GSIS in islets from ABHD6-KO, heterozygote (HZ), and wild-type (WT) mice. GSIS was measured at basal (2.8G), intermediate (8.3G) and high (16.7G) glucose concentrations (n = 6 mice per group); *p < 0.05; **p < 0.01; ***p < 0.001 versus WT group at the same glucose concentration.

(C) Total MAG content of islets from ABHD6-KO, HZ, and WT mice. Isolated islets were incubated at 2.8 mM (2.8G) and 16.7 mM (16.7G) glucose for 1 hr in KRBH, and islet MAG levels were analyzed (n = 3). *p < 0.05 versus 2.8G in the same genotype; ##p < 0.01 versus WT islets.

(D) Total 1-MAG levels in the islets incubated as in (B) (n = 3). **p < 0.01 versus 2.8G in the same genotype; ##p < 0.01 versus WT islets.

(E–G) Effect of ABHD6 gene knockout in male mice on glucose-induced insulin secretion and insulin sensitivity.

(E) Glycemia during oral glucose tolerance test (OGTT) in 26-week-old WT, HZ, and KO mice (n = 5–8 per group). OGTT was performed after a 6 hr food withdrawal. Inset, area under the curve (AUC).

(F) Corresponding insulinemia; inset, AUC. *p < 0.05 versus WT.

(G) Insulin sensitivity assessment by hyperinsulinemic euglycemic clamp in 26-week-old chow-fed ABHD6-KO male mice. Glycemia was clamped at 7.2 mM, and glucose infusion rate was calculated and shown as inset for 90 to 120 min time period of the clamp.

(H–K) Effect of in vivo pharmacological suppression of ABHD6 by WWL70 on glucose-induced insulin secretion in normal and diabetic mice. Diabetes was induced in CD1 mice by a single low-dose of streptozotocin. After 4 weeks, the diabetic and control mice were treated daily with WWL70 (i.p., 5 mg/kg BW) or vehicle for 3 days, followed by OGTT (8–10 mice per group).

(H and I) (H) Glycemia and (I) insulinemia in normal mice. Insets depict AUC. *p < 0.05; **p < 0.01 versus vehicle treated.

(J and K) (J) Glycemia and (K) insulinemia in STZ diabetic mice. Insets depict AUC. *p < 0.05; **p < 0.01 versus vehicle treated. All the values shown are mean ±SEM.

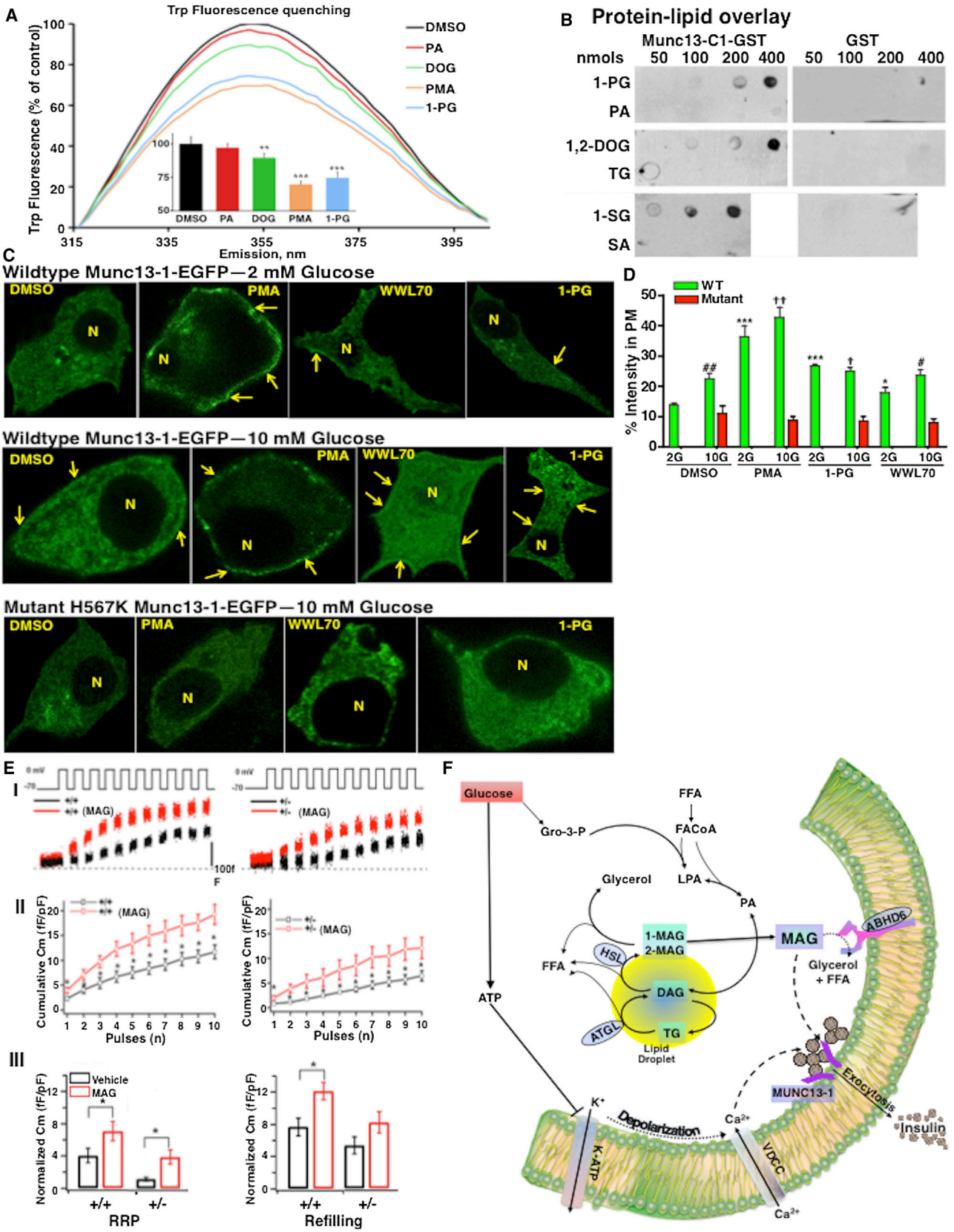

(legend on next page)

promotes the translocation of Munc13-1-EGFP to plasma membrane, and this translocation is not seen with H567K mutant Munc13-1-EGFP (mutation in the DAG-binding C1 domain). PMA caused much higher Munc13-1 translocation, independent of glucose levels. ABHD6 inhibitor WWL70, which increases intracellular MAG levels, and exogenous 1-PG caused significantly increased translocation of Munc13-1 at 10 mM glucose and to a lesser extent at 2 mM glucose (Figures 7C and 7D). These effects were lost with H567K mutant Munc13-1. In a complementary approach, we noticed that in WT islets, high glucose increased Munc13-1 translocation to a membrane fraction. In addition, incubation of whole-body ABHD6-KO mouse islets at high glucose (which elevates their MAG levels; see Figures 5C and 5D) led to a greater increased Munc13-1 migration to plasma membrane in comparison to WT mouse islets and also to KO islets incubated at low glucose concentration (Figure S6B). These results further support the view that MAG binds with Munc13-1 at its C1 domain, in situ, and causes its translocation to plasma membrane, an important step in insulin granule exocytosis.

MAG Directly Promotes Exocytosis in Single β Cells at Least in Part via Munc13-1

We examined whether MAG promotes exocytosis by acting on Munc13-1 by performing cell membrane capacitance (Cm) measurements by patch clamp, using islet β cells from *Munc13-1*$^{+/+}$ and *Munc13-1*$^{+/-}$ mice (*Munc13-1*$^{-/-}$ mice are not viable). Insulin exocytosis was induced by a train of ten 500 ms depolarization pulses. Cell Cm changes elicited by the first two pulses approximate the size of the ready releasable pool (RRP) of primed and fusion-ready granules, reflecting the first phase insulin secretion. Subsequent pulses estimate the rate of granule refilling or mobilization from the reserve pool(s) to the RRP (Gillis et al., 1996), which correlates with the second phase of insulin secretion (Rorsman and Renström, 2003). In *Munc13-1*$^{+/+}$ β cells, 1-PG increased Cm at every depolarizing pulse (Figure 7E) and enhanced insulin exocytosis in both the size of RRP and the rate of granule pool refilling compared with control. In *Munc13-1*$^{+/-}$ β cells exocytosis was reduced by ~50%, and MAG stimulation of exocytosis was also decreased proportionally. While 1-PG could significantly enhance insulin exocytosis in the RRP in *Munc13-1*$^{+/-}$ β cells, the rate of refilling was not significantly stimulated, unlike in the *Munc13-1*$^{+/+}$ β cells.

We examined if MAG affects voltage-gated Ca^{2+} channel activity, which plays key role in GSIS (Prentki and Matschinsky, 1987; Rorsman and Renström, 2003). In the β cells from both *Munc13*$^{+/+}$ and *Munc13*$^{+/-}$ mice, no significant changes in Ca^{2+} current amplitudes and current densities were observed with or without MAG or WWL70 pretreatment (Figure S6C).

Recent studies (Iwasaki et al., 2008; Zygmunt et al., 2013) suggested that MAG activates the transient receptor potential vanilloid-1 (TRPV1), which when stimulated acts as a Ca^{2+} channel. We examined this possibility by employing a pharmacological antagonist AMG9810 and TRPV1-KO mice for both in vivo and ex vivo studies. The results ruled out this possibility (data not shown).

DISCUSSION

This study provides biochemical, pharmacological, cell biology, and genetic evidence in support of the hypothesis, depicted in Figure S6D, proposing that the enigmatic lipolysis-derived molecule mediating the link between glucose metabolism and insulin granule exocytosis in the β cell is MAG that targets Munc13-1 and that the signaling competent MAG level is controlled by ABHD6. The overwhelming set of data and complementary approaches that collectively support this view are summarized as follows: (1) GSIS is reduced both in vivo and *ex-vivo* in mice deficient in ATGL (Peyot et al., 2009) and HSL (Fex et al., 2009; Peyot et al., 2004), the first two enzymes of the lipolysis pathway. (2) Elevated glucose promotes β cell lipolysis, as shown by a rise FFA levels inside and released from β cells. (3) GSIS in INS832/13 cells is associated with a rise in total MAG levels, in particular, saturated FA containing 1-MAG. (4) Exogenous MAG amplifies GSIS in INS832/13 cells and islet tissues. (5) GSIS is curtailed by the panlipase inhibitor orlistat, which suppresses lipolysis and the glucose-induced rise in MAG. (6) Orlistat-inhibited GSIS is restored by exogenous MAG. (7) ABHD6 is expressed at high levels in the β cell and islet tissues, whereas MAGL is poorly expressed. (8) The ABHD6 inhibitor WWL70 enhances glucose-induced MAG accumulation and insulin secretion.

Figure 7. Monoacylglycerol Binds to Munc13-1 C1 Domain, Facilitates Munc13-1 Translocation to Plasma Membrane, and Stimulates Insulin Exocytosis in Single β Cells

(A) Ligand binding to Munc13-1 C1 domain assessed by tryptophan fluorescence quenching. Representative fluorescence emission spectra of Munc13-1 C1 peptide (1 μM) incubated with 1 μM of either palmitic acid (PA), 1,2-dioctanoylglycerol (DOG), phorbol-12-myristate-13-acetate (PMA), or 1-PG or DMSO. Inset: peak fluorescence emission at 350 nm; n = 3 experiments, each with ten spectra. **p < 0.001 and ***p < 0.00001.

(B) Protein-lipid overlay assay. 1-PG, PA, 1,2-DOG, triglycerides (TG), 1-SG, and stearic acid (SA) were spotted on nitrocellulose membrane and, after blocking, membranes were incubated with 10 μg/ml of Munc13-1-C1-GST fusion protein or GST (negative control) and processed as described in Experimental Procedures for assessing the bound Munc13-1-C1-GST.

(C) INS832/13 cells were transfected with plasmids expressing either pEGFP-WT Munc13-1 or pEGFP-H567K mutant Munc13-1 and were grown on coverslips. Three days later, the cells were incubated in KRBH at 2 or 10 mM glucose, containing 0.3 μM PMA, 10 μM WWL70, 100 μM 1-PG, or DMSO for 10 min at 37°C. Then the coverslips were processed and imaged using confocal microscope. Representative images are shown.

(D) Munc13-1 translocation to plasma membrane was quantified using Image J software. About six to ten individual cells were imaged per each treatment. Results are expressed as pixel intensity in the plasma membrane as a percentage of whole-cell intensity. *p < 0.05 and ***p < 0.001 versus 2G DMSO control; #p < 0.05 and ##p < 0.01 versus corresponding 2G control; †p < 0.05 and ††p < 0.01 versus 10G DMSO control. Details in Supplemental Information.

(E) MAG induction of exocytosis is dependent on Munc13-1. Changes in cell membrane capacitance (Cm) were measured in *Munc13-1*$^{+/+}$ and *Munc13-1*$^{+/-}$ mice β cells with or without 1-PG (MAG) pretreatment using a train of ten depolarization pulses (500 ms in duration) from −70 mV to 0 mV. Panel I: representative recordings of exocytosis from *Munc13-1*$^{+/+}$ and *Munc13*$^{+/-}$ mice β cells with or without MAG pretreatment. Panel II: cumulative changes in cell capacitance normalized to basal cell membrane capacitance (fF/pF) in *Munc13-1*$^{+/+}$ and *Munc13-1*$^{+/-}$ mice β cells with or without MAG pretreatment (n = 11–16 cells, from three to four mice). *p < 0.05. Panel III: statistical analysis showing the size of the readily releasable pool (RRP) of insulin granules and the rate of granule mobilization (refilling) (n = 11–16 cells, from three to four mice). *p < 0.05. All the values shown are mean ±SEM.

(9) Overexpression of ABHD6 in the β cell reduces GSIS, whereas RNAi silencing of the enzyme enhances insulin release. (10) Islets from whole-body ABHD6-KO mouse show elevated GSIS ex vivo. (11) MAG hydrolyzing activity of ABHD6-KO islets is reduced by ~50%, and the remaining activity is insensitive to inhibition by WWL70. (12) The enhanced GSIS seen in ABHD6-KO mouse islets ex vivo is not further increased by ABHD6 inhibitor WWL70. (13) While total and 1-MAG levels increase in islets from ABHD6-KO, HZ, and WT mice at high glucose concentration, this increase is inversely proportional to "ABHD6-gene dosage." (14) GSIS in vivo is enhanced in whole-body ABHD6-deficient mice. (15) β-cell-specific deletion of ABHD6 in mice also led to enhanced GSIS both in vivo and in islets ex vivo, thus excluding any involvement of central nervous system or peripheral tissues in the enhanced GSIS. (16) WWL70 enhances GSIS in vivo in control mice and restores GSIS in LD-STZ diabetic mice. (17) MAG binds efficiently to the exocytotic effector Munc13-1. (18) Addition of either WWL70 or exogenous MAG increased the glucose-stimulated translocation of Munc13-1 to plasma membrane in INS832/13 β cells, and this effect is lost with C1-domain-mutated Munc13-1. (19) Glucose stimulation of ABHD6-KO mouse islets caused increased migration of Munc13-1 to plasma membrane. (20) MAG causes exocytosis in single patch-clamped β cells. (21) MAG-induced exocytosis is reduced in *Munc13-1*$^{+/-}$ β cells.

Saturated long-chain 1-MAG (e.g., 1-PG or 1-SG) is likely the physiologically relevant MAG with regard to metabolic coupling for GSIS. Thus, glucose stimulation and suppression of ABHD6 either by its inhibition by WWL 70 or its genetic deletion caused more prominent rises in saturated 1-MAG than 2-MAG species. In addition, glucose only triggered the release of lipolysis-derived, saturated long-chain FAs. Furthermore, saturated long-chain fatty acyl 1-MAGs were better secretagogues than monounsaturated or polyunsaturated 1-MAG species. In addition, elevated glucose caused a prominent rise in the incorporation of labeled glucose into 1-MAG, whereas incorporation into 2-MAG was largely unaltered. Also, the lipolysis inhibitor orlistat suppressed the impact of glucose on 1-MAG levels but barely affected the incorporation of glucose into 2-MAG or DAG. These findings are completely congruent with the fact that lipolysis of TG by ATGL generates primarily 1,3-DAG (Eichmann et al., 2012; Lass et al., 2011), which is further hydrolyzed to 1-MAG by HSL. Interestingly, a recent study documented that ABHD6 has preferential activity for 1-MAG species, and saturated long-chain 1-MAG species are efficiently hydrolyzed by the enzyme (Navia-Paldanius et al., 2012). Although ABHD6 was reported in a recent study to hydrolyze lysophosphatidylglycerol (Thomas et al., 2013), this activity is only about 5% of this enzyme's MAG hydrolyzing activity, indicating that ABHD6 is predominantly a MAG hydrolase.

The results indicate that there is a "signaling competent pool" of 1-MAG, likely close to or associated to the inner side of the plasma membrane that plays a role in insulin exocytosis. ABHD6 controls the level of this pool, thereby regulating GSIS, whereas this pool of 1-MAG is not influenced by MAGL, which per se is expressed at low levels in β cells. Thus, using pharmacological and siRNA agents, we observed that ABHD6 inhibition, but not MAGL inhibition, alters GSIS. Notably, MAGL is an amphiphilic enzyme distributed between cytosol and membrane fractions (Severson and Hee-Cheong, 1988), whereas ABHD6 is exclusively membrane bound (Marrs et al., 2010). Similar intracellular compartmentalization having an impact on the signaling functions of eicosanoids (Bozza et al., 2011) and sphingolipids (Siow and Wattenberg, 2011), because of the intracellular distribution of the involved enzymes, has been described.

We ruled out the possibility that endocannabinoid receptors (Matias et al., 2006) that bind 2-arachidonoylglycerol, but not saturated MAG, are involved in the MAG-mediated effects on insulin secretion. Thus, a specific antagonist of the CB1 receptor (AM251) (Lan et al., 1999) and an inverse agonist (AM630) of the CB2 receptor (Ross et al., 1999) did not alter GSIS. In addition, the restoration of orlistat-inhibited GSIS by 2-AG was not affected by AM251. Finally, 2-AG levels even at high glucose were <1% of the total β cell MAG, whereas the saturated MAG that rose in the presence of glucose was 100-fold higher, as compared to 2-arachidonylglycerol and stimulated insulin secretion. Noteworthy, only 2-AG, but not saturated MAG, can bind CB receptors and act as their ligand (Ben-Shabat et al., 1998). It was earlier suggested (Li et al., 2012) that MAGL is important in GSIS regulation in MIN6 cells and islets by regulating 2-AG levels. However, these authors employed URB602, which has low affinity for MAGL (Ki ~28 μM) and is not selective (Vandevoorde et al., 2007; Wiskerke et al., 2012). In fact, URB602 at 50 μM caused glucose-independent insulin secretion (at 2 mM glucose) and reduced GSIS at 20 mM glucose (Li et al., 2012), a clear indication of this drug's toxic effects on β cell. In our studies, we employed 1 μM JZL184 (IC_{50} 25 nM for rat MAGL; Long et al., 2009) to inhibit MAGL, which does not exert any toxic effects, and our results rule out the involvement of CB1/2 receptors in GSIS regulation.

Since the components of exocytotic machinery, including Munc13-1, are needed also for non-fuel-induced insulin secretion (e.g., high KCl) (Roduit et al., 2004), it is anticipated that elevated levels of MAG can influence KCl-induced secretion via Munc13-1 activation. Thus, in the islets from ABHD6-KO mice, the elevated secretion by KCl (at 2.8 mM glucose) could be due to increased MAG levels even at 2.8 mM glucose in these islets. However, in INS832/13 cells, ABHD6 inhibition by WWL70 had no effect on KCl-induced secretion (at 1 mM glucose), as under these conditions, MAG levels did not increase in these cells.

How is MAG signaling linked to insulin secretion? Munc-13-1, a vesicle priming protein (Kwan et al., 2006; Sheu et al., 2003), was proposed to be activated upon DAG binding to its C1 domain (Rhee et al., 2002) and to translocate to plasma membrane and promote insulin granule exocytosis (Kwan et al., 2006; Sheu et al., 2003). However, NMR studies revealed that DAG binds with low affinity to Munc13-1 due to an occluding tryptophan residue in the C1 domain (Shen et al., 2005). We now demonstrate that the C1 domain of Munc13-1 binds to MAG more efficiently than to DAG. Hence, the accumulation of MAG at high glucose likely results in the activation of Munc13-1 and exocytosis. Inasmuch as high glucose and also ABHD6 inhibition lead to much higher rise in 1-MAG levels than in total DAG, and because orlistat, which suppresses GSIS completely, reduces MAG but not DAG in β cells, MAG rather than DAG is the more plausible activator of Munc13-1

linked to insulin exocytosis. WT Munc13-1, but not the C1 domain mutant (H567K) Munc13-1, showed glucose-stimulated translocation to plasma membrane and exogenous MAG or the ABHD6 inhibitor WWL70 also increased Munc13-1 translocation to the plasma membrane to the same extent as high glucose, which strongly implicates MAG as the physiological modulator of Munc13-1 migration. We further found in patch clamp experiments in WT β cells that 1-PG increases exocytosis from granules located in both the readily releasable and reserve/refilling pools that correspond to first- and second-phase GSIS, respectively. Exocytosis from granules derived from the two pools was reduced in *Munc13*$^{+/-}$β cells both in the absence and presence of MAG, again supporting the view that Munc13-1 is a target of MAG action.

Overall, the present study identifies MAG (in particular, long-chain saturated 1-MAG species) as a lipid metabolic coupling factor linking glucose metabolism in the pancreatic islet β cell to insulin secretion. MAG appears to target at least in part Munc13-1, a key exocytotic effector that orchestrates membrane fusion events. The results also show that the MAG signal for insulin secretion is modulated by the membrane-bound MAG hydrolase ABHD6. Identifying MAG species other than the endocannabinoid 2-AG as signaling molecules may prove to be of broad significance in various cell types and diseases. In addition, it will be of interest to determine whether ABHD6 inhibition may provide a useful approach to develop antidiabetic agents and insulin secretagogues.

EXPERIMENTAL PROCEDURES

Islet Isolation

Pancreatic islets were isolated from male Wistar rats, C57Bl6, or CD1 mice as before (Peyot et al., 2009). Human islets (75 to 90% pure) were from Beta-Pro LLC (Virginia).

Insulin Secretion in Isolated Islets and INS832/13 Cells

Insulin secretion (Hohmeier et al., 2000) was measured in static incubations as described earlier (Peyot et al., 2009) in the absence or presence of the pharmacological agents WWL70, orlistat, and JZL184.

Overexpression and RNAi Knockdown of ABHD6 and MAGL

The pCMV plasmids expressing human ABHD6, MAGL, and GFP were from Origene. pCMV-AC plasmids coding for either ABHD6, MAGL, or GFP (control) were introduced into INS832/13 cells using Amaxa Nucleofector (Program T-27, solution V; Amaxa Inc). After transfection, cells were cultured for 72 hr in 12-well and 6-well plates for insulin secretion and western blot analysis, respectively. Silencer select siRNA against ABHD6 and two scrambled siRNA were from Ambion. For RNAi knockdown of MAGL, two siRNA were used. siRNA constructs were introduced into INS832/13 cells using RNAiMAX (Invitrogen) and used 24 hr after transfection for western blotting and insulin secretion determination.

Effect of ABHD6 Inhibitor in LD-STZ Mouse Diabetes Model

In vivo efficacy of the ABHD6 inhibitor WWL70 was assessed in a LD-STZ type 2 diabetes mouse model with impaired insulin secretion and reduced β cell mass (Hayashi et al., 2006).

Analysis of MAG Binding to Munc13-1 C1 Domain

Rat Munc13-1 C1 domain (residues 567–617) was cloned as GST fusion protein (Shen et al., 2005) and was expressed in *E. coli*, and the C1-peptide was purified after thrombin cleavage. Synthetic rat Munc13-1-C1 peptide was from Biomatik. MAG binding to Munc13-C1 domain was assessed by the following: (1) tryptophan fluorescence quenching; (2) 1-(12-(7-Nitrobenz-2-oxa-1,3-diazol-4-yl)amino)dodecanoylglycerol (NBD-MAG) fluorescence quenching, and (3) protein-lipid overlay.

Assessment of MAG-Induced Munc13-1 Translocation, In Situ, in INS832/13 Cells

INS832/13 cells were transfected with plasmids expressing either Munc13-1-EGFP or H567K mutant Munc13-1-EGFP and plated on coverslips. After 48 hr, the cells were incubated at 2 and 10 mM glucose, with and without 1 μM PMA, 10 μM WWL70, or 100 μM 1-PG, for 10 min and were processed for confocal microscopy.

Studies in *Munc13-1*$^{+/-}$ Mouse Islets

Munc13-1$^{+/-}$ mouse (Augustin et al., 1999; Rhee et al., 2002) islets were isolated as described before (Kwan et al., 2006) and dispersed into single cells that were plated on glass coverslips and allowed to adhere for 48 hr before cell capacitance measurements.

ABHD6 KO Mice

Whole-body and BKO mice were generated by employing "KO-first" design (Skarnes et al., 2011). The mice used were of pure C57/BL6N background and the ES cells (JM8A3.N1 [Agouti], also derived from C57Bl6N) with confirmed conditional vector targeting for ABHD6 (HEPD0651_8_C07) were obtained from European Conditional Mouse Mutagenesis Program (Germany). Details are given in Supplemental Experimental Procedures.

Determination of FFA and Monoacylglycerol Species

FFAs accumulated in the rat islets and INS832/13 cells and released into the medium were extracted, derivatized with phenacylbromide, and quantified by reverse phase HPLC. Total lipids from rat islets and INS832/13 cells were extracted, separated on boric acid/silica gel thin-layer chromatography (TLC) with two solvent systems to allow 1- and 2-MAG separation. The separated 1- and 2-MAG spots were scraped from the TLC plates and used to determine different MAG species, with respect to the attached FA by saponification and extraction in n-heptane, followed by quantification by reverse-phase HPLC.

Statistical Analysis

Values are expressed as mean ±SEM. Statistical analysis was performed using one-way ANOVA with Dunnett's post hoc test for multiple comparisons or two-way ANOVA with Bonferroni's post hoc test for multiple comparisons using GraphPad Prism. For electrophysiology experiments, comparisons were by unpaired two-tailed Student's t test.

SUPPLEMENTAL INFORMATION

Supplemental Information includes six figures and Supplemental Experimental Procedures and can be found with this article online at http://dx.doi.org/10.1016/j.cmet.2014.04.003.

AUTHOR CONTRIBUTIONS

S.Z., Y.M., and J.I. conceived and performed the experiments and analyzed data. L.I. and H.G. performed patch-clamp experiments and analyzed the data. V.D-A. and R..L. performed in vitro experiments. M-L.P. and E.J. helped analysis of results and discussion. B.T. helped in the experiments related to hypothalamic regions. M.A.D., J.M.B., and A.A. contributed reagents. S.R.M.M. and M.P. conceived the project, designed the study, analyzed the results, and wrote the manuscript.

ACKNOWLEDGMENTS

This work was supported by grants from the Canadian Institutes of Health Research (M.P. and S.R.M.M.). M.P. holds the Canada Research Chair in Diabetes and Metabolism. H.G. is supported by grants from the Canadian Institutes of Health Research. S.Z. was supported by studentships from Diabète Québec and the Montreal Diabetes Research Center. Y.M. was supported by studentships from the Fonds de Recherche Québec-Santé, the department of Nutrition of Université de Montréal, and Diabète Québec, and B.T. received

a fellowship from Diabète Québec. We thank Robert Zimmermann, Christopher Nolan, Vincent Poitout, Robert Farese, Jr., and Stephanie Fulton for critical review of the manuscript. We thank Dr. Thierry Alquier for his advice for isolation of hypothalamic regions and Dr. Josep Rizo, University of Texas, for a gift of Munc13-1-C1-GST expression plasmid.

Received: June 6, 2013
Revised: January 24, 2014
Accepted: March 26, 2014
Published: May 8, 2014

REFERENCES

Alhouayek, M., Masquelier, J., Cani, P.D., Lambert, D.M., and Muccioli, G.G. (2013). Implication of the anti-inflammatory bioactive lipid prostaglandin D2-glycerol ester in the control of macrophage activation and inflammation by ABHD6. Proc. Natl. Acad. Sci. USA *110*, 17558–17563.

Ashcroft, F.M., and Rorsman, P. (2012). Diabetes mellitus and the β cell: the last ten years. Cell *148*, 1160–1171.

Augustin, I., Rosenmund, C., Südhof, T.C., and Brose, N. (1999). Munc13-1 is essential for fusion competence of glutamatergic synaptic vesicles. Nature *400*, 457–461.

Bachovchin, D.A., Ji, T., Li, W., Simon, G.M., Blankman, J.L., Adibekian, A., Hoover, H., Niessen, S., and Cravatt, B.F. (2010). Superfamily-wide portrait of serine hydrolase inhibition achieved by library-versus-library screening. Proc. Natl. Acad. Sci. USA *107*, 20941–20946.

Ben-Shabat, S., Fride, E., Sheskin, T., Tamiri, T., Rhee, M.H., Vogel, Z., Bisogno, T., De Petrocellis, L., Di Marzo, V., and Mechoulam, R. (1998). An entourage effect: inactive endogenous fatty acid glycerol esters enhance 2-arachidonoyl-glycerol cannabinoid activity. Eur. J. Pharmacol. *353*, 23–31.

Blankman, J.L., Simon, G.M., and Cravatt, B.F. (2007). A comprehensive profile of brain enzymes that hydrolyze the endocannabinoid 2-arachidonoylglycerol. Chem. Biol. *14*, 1347–1356.

Bozza, P.T., Bakker-Abreu, I., Navarro-Xavier, R.A., and Bandeira-Melo, C. (2011). Lipid body function in eicosanoid synthesis: an update. Prostaglandins Leukot. Essent. Fatty Acids *85*, 205–213.

Eichmann, T.O., Kumari, M., Haas, J.T., Farese, R.V., Jr., Zimmermann, R., Lass, A., and Zechner, R. (2012). Studies on the substrate and stereo/regioselectivity of adipose triglyceride lipase, hormone-sensitive lipase, and diacylglycerol-O-acyltransferases. J. Biol. Chem. *287*, 41446–41457.

Eliasson, L., Abdulkader, F., Braun, M., Galvanovskis, J., Hoppa, M.B., and Rorsman, P. (2008). Novel aspects of the molecular mechanisms controlling insulin secretion. J. Physiol. *586*, 3313–3324.

Fex, M., Haemmerle, G., Wierup, N., Dekker-Nitert, M., Rehn, M., Ristow, M., Zechner, R., Sundler, F., Holm, C., Eliasson, L., and Mulder, H. (2009). A beta cell-specific knockout of hormone-sensitive lipase in mice results in hyperglycaemia and disruption of exocytosis. Diabetologia *52*, 271–280.

Gillis, K.D., Mossner, R., and Neher, E. (1996). Protein kinase C enhances exocytosis from chromaffin cells by increasing the size of the readily releasable pool of secretory granules. Neuron *16*, 1209–1220.

Green, C.D., Jump, D.B., and Olson, L.K. (2009). Elevated insulin secretion from liver X receptor-activated pancreatic beta-cells involves increased de novo lipid synthesis and triacylglyceride turnover. Endocrinology *150*, 2637–2645.

Guenifi, A., Simonsson, E., Karlsson, S., Ahrén, B., and Abdel-Halim, S.M. (2001). Carbachol restores insulin release in diabetic GK rat islets by mechanisms largely involving hydrolysis of diacylglycerol and direct interaction with the exocytotic machinery. Pancreas *22*, 164–171.

Haemmerle, G., Zimmermann, R., Hayn, M., Theussl, C., Waeg, G., Wagner, E., Sattler, W., Magin, T.M., Wagner, E.F., and Zechner, R. (2002). Hormone-sensitive lipase deficiency in mice causes diglyceride accumulation in adipose tissue, muscle, and testis. J. Biol. Chem. *277*, 4806–4815.

Hayashi, K., Kojima, R., and Ito, M. (2006). Strain differences in the diabetogenic activity of streptozotocin in mice. Biol. Pharm. Bull. *29*, 1110–1119.

Henquin, J.C. (2011). The dual control of insulin secretion by glucose involves triggering and amplifying pathways in β-cells. Diabetes Res. Clin. Pract. *93* (*Suppl 1*), S27–S31.

Hohmeier, H.E., Mulder, H., Chen, G., Henkel-Rieger, R., Prentki, M., and Newgard, C.B. (2000). Isolation of INS-1-derived cell lines with robust ATP-sensitive K+ channel-dependent and -independent glucose-stimulated insulin secretion. Diabetes *49*, 424–430.

Iwasaki, Y., Saito, O., Tanabe, M., Inayoshi, K., Kobata, K., Uno, S., Morita, A., and Watanabe, T. (2008). Monoacylglycerols activate capsaicin receptor, TRPV1. Lipids *43*, 471–483.

Jitrapakdee, S., Wutthisathapornchai, A., Wallace, J.C., and MacDonald, M.J. (2010). Regulation of insulin secretion: role of mitochondrial signalling. Diabetologia *53*, 1019–1032.

Kim, W., Doyle, M.E., Liu, Z., Lao, Q., Shin, Y.K., Carlson, O.D., Kim, H.S., Thomas, S., Napora, J.K., Lee, E.K., et al. (2011). Cannabinoids inhibit insulin receptor signaling in pancreatic β-cells. Diabetes *60*, 1198–1209.

Kwan, E.P., and Gaisano, H.Y. (2009). Rescuing the subprime meltdown in insulin exocytosis in diabetes. Ann. N Y Acad. Sci. *1152*, 154–164.

Kwan, E.P., Xie, L., Sheu, L., Nolan, C.J., Prentki, M., Betz, A., Brose, N., and Gaisano, H.Y. (2006). Munc13-1 deficiency reduces insulin secretion and causes abnormal glucose tolerance. Diabetes *55*, 1421–1429.

Lan, R., Liu, Q., Fan, P., Lin, S., Fernando, S.R., McCallion, D., Pertwee, R., and Makriyannis, A. (1999). Structure-activity relationships of pyrazole derivatives as cannabinoid receptor antagonists. J. Med. Chem. *42*, 769–776.

Lass, A., Zimmermann, R., Oberer, M., and Zechner, R. (2011). Lipolysis - a highly regulated multi-enzyme complex mediates the catabolism of cellular fat stores. Prog. Lipid Res. *50*, 14–27.

Li, C., Vilches-Flores, A., Zhao, M., Amiel, S.A., Jones, P.M., and Persaud, S.J. (2012). Expression and function of monoacylglycerol lipase in mouse β-cells and human islets of Langerhans. Cell. Physiol. Biochem. *30*, 347–358.

Long, J.Z., Nomura, D.K., and Cravatt, B.F. (2009). Characterization of monoacylglycerol lipase inhibition reveals differences in central and peripheral endocannabinoid metabolism. Chem. Biol. *16*, 744–753.

Ma, C., Su, L., Seven, A.B., Xu, Y., and Rizo, J. (2013). Reconstitution of the vital functions of Munc18 and Munc13 in neurotransmitter release. Science *339*, 421–425.

MacDonald, P.E. (2011). Signal integration at the level of ion channel and exocytotic function in pancreatic β-cells. Am. J. Physiol. Endocrinol. Metab. *301*, E1065–E1069.

Maechler, P., and Wollheim, C.B. (1998). Role of mitochondria in metabolism-secretion coupling of insulin release in the pancreatic beta-cell. Biofactors *8*, 255–262.

Marrs, W.R., Blankman, J.L., Horne, E.A., Thomazeau, A., Lin, Y.H., Coy, J., Bodor, A.L., Muccioli, G.G., Hu, S.S., Woodruff, G., et al. (2010). The serine hydrolase ABHD6 controls the accumulation and efficacy of 2-AG at cannabinoid receptors. Nat. Neurosci. *13*, 951–957.

Matias, I., Gonthier, M.P., Orlando, P., Martiadis, V., De Petrocellis, L., Cervino, C., Petrosino, S., Hoareau, L., Festy, F., Pasquali, R., et al. (2006). Regulation, function, and dysregulation of endocannabinoids in models of adipose and beta-pancreatic cells and in obesity and hyperglycemia. J. Clin. Endocrinol. Metab. *91*, 3171–3180.

Navia-Paldanius, D., Savinainen, J.R., and Laitinen, J.T. (2012). Biochemical and pharmacological characterization of human α/β-hydrolase domain containing 6 (ABHD6) and 12 (ABHD12). J. Lipid Res. *53*, 2413–2424.

Nolan, C.J., and Prentki, M. (2008). The islet beta-cell: fuel responsive and vulnerable. Trends Endocrinol. Metab. *19*, 285–291.

Nolan, C.J., Leahy, J.L., Delghingaro-Augusto, V., Moibi, J., Soni, K., Peyot, M.L., Fortier, M., Guay, C., Lamontagne, J., Barbeau, A., et al. (2006a). Beta cell compensation for insulin resistance in Zucker fatty rats: increased lipolysis and fatty acid signalling. Diabetologia *49*, 2120–2130.

Nolan, C.J., Madiraju, M.S., Delghingaro-Augusto, V., Peyot, M.L., and Prentki, M. (2006b). Fatty acid signaling in the beta-cell and insulin secretion. Diabetes *55* (*Suppl 2*), S16–S23.

Peyot, M.L., Nolan, C.J., Soni, K., Joly, E., Lussier, R., Corkey, B.E., Wang, S.P., Mitchell, G.A., and Prentki, M. (2004). Hormone-sensitive lipase has a role in lipid signaling for insulin secretion but is nonessential for the incretin action of glucagon-like peptide 1. Diabetes *53*, 1733–1742.

Peyot, M.L., Guay, C., Latour, M.G., Lamontagne, J., Lussier, R., Pineda, M., Ruderman, N.B., Haemmerle, G., Zechner, R., Joly, E., et al. (2009). Adipose triglyceride lipase is implicated in fuel- and non-fuel-stimulated insulin secretion. J. Biol. Chem. *284*, 16848–16859.

Prentki, M., and Madiraju, S.R. (2012). Glycerolipid/free fatty acid cycle and islet β-cell function in health, obesity and diabetes. Mol. Cell. Endocrinol. *353*, 88–100.

Prentki, M., and Matschinsky, F.M. (1987). Ca2+, cAMP, and phospholipid-derived messengers in coupling mechanisms of insulin secretion. Physiol. Rev. *67*, 1185–1248.

Prentki, M., Matschinsky, F.M., and Madiraju, S.R. (2013). Metabolic signaling in fuel-induced insulin secretion. Cell Metab. *18*, 162–185.

Rhee, J.S., Betz, A., Pyott, S., Reim, K., Varoqueaux, F., Augustin, I., Hesse, D., Südhof, T.C., Takahashi, M., Rosenmund, C., and Brose, N. (2002). Beta phorbol ester- and diacylglycerol-induced augmentation of transmitter release is mediated by Munc13s and not by PKCs. Cell *108*, 121–133.

Roduit, R., Nolan, C., Alarcon, C., Moore, P., Barbeau, A., Delghingaro-Augusto, V., Przybykowski, E., Morin, J., Massé, F., Massie, B., et al. (2004). A role for the malonyl-CoA/long-chain acyl-CoA pathway of lipid signaling in the regulation of insulin secretion in response to both fuel and nonfuel stimuli. Diabetes *53*, 1007–1019.

Rorsman, P., and Renström, E. (2003). Insulin granule dynamics in pancreatic beta cells. Diabetologia *46*, 1029–1045.

Ross, R.A., Brockie, H.C., Stevenson, L.A., Murphy, V.L., Templeton, F., Makriyannis, A., and Pertwee, R.G. (1999). Agonist-inverse agonist characterization at CB1 and CB2 cannabinoid receptors of L759633, L759656, and AM630. Br. J. Pharmacol. *126*, 665–672.

Severson, D.L., and Hee-Cheong, M. (1988). Monoacylglycerol lipase activity in cardiac myocytes. Biochem. Cell Biol. *66*, 1013–1018.

Shen, N., Guryev, O., and Rizo, J. (2005). Intramolecular occlusion of the diacylglycerol-binding site in the C1 domain of munc13-1. Biochemistry *44*, 1089–1096.

Sheu, L., Pasyk, E.A., Ji, J., Huang, X., Gao, X., Varoqueaux, F., Brose, N., and Gaisano, H.Y. (2003). Regulation of insulin exocytosis by Munc13-1. J. Biol. Chem. *278*, 27556–27563.

Siow, D., and Wattenberg, B. (2011). The compartmentalization and translocation of the sphingosine kinases: mechanisms and functions in cell signaling and sphingolipid metabolism. Crit. Rev. Biochem. Mol. Biol. *46*, 365–375.

Skarnes, W.C., Rosen, B., West, A.P., Koutsourakis, M., Bushell, W., Iyer, V., Mujica, A.O., Thomas, M., Harrow, J., Cox, T., et al. (2011). A conditional knockout resource for the genome-wide study of mouse gene function. Nature *474*, 337–342.

Thomas, G., Betters, J.L., Lord, C.C., Brown, A.L., Marshall, S., Ferguson, D., Sawyer, J., Davis, M.A., Melchior, J.T., Blume, L.C., et al. (2013). The serine hydrolase ABHD6 Is a critical regulator of the metabolic syndrome. Cell Rep. *5*, 508–520.

Vandevoorde, S., Jonsson, K.O., Labar, G., Persson, E., Lambert, D.M., and Fowler, C.J. (2007). Lack of selectivity of URB602 for 2-oleoylglycerol compared to anandamide hydrolysis in vitro. Br. J. Pharmacol. *150*, 186–191.

Wicksteed, B., Brissova, M., Yan, W., Opland, D.M., Plank, J.L., Reinert, R.B., Dickson, L.M., Tamarina, N.A., Philipson, L.H., Shostak, A., et al. (2010). Conditional gene targeting in mouse pancreatic ß-Cells: analysis of ectopic Cre transgene expression in the brain. Diabetes *59*, 3090–3098.

Wiskerke, J., Irimia, C., Cravatt, B.F., De Vries, T.J., Schoffelmeer, A.N., Pattij, T., and Parsons, L.H. (2012). Characterization of the effects of reuptake and hydrolysis inhibition on interstitial endocannabinoid levels in the brain: an in vivo microdialysis study. ACS Chem. Neurosci. *3*, 407–417.

Zygmunt, P.M., Ermund, A., Movahed, P., Andersson, D.A., Simonsen, C., Jönsson, B.A., Blomgren, A., Birnir, B., Bevan, S., Eschalier, A., et al. (2013). Monoacylglycerols activate TRPV1—a link between phospholipase C and TRPV1. PLoS ONE *8*, e81618.